

Redox gradient shapes the abundance and diversity of mercury-methylating microorganisms along the water column of the Black Sea

Léa Cabrol,^{1,2} Eric Capo,^{3,4,5} Daan M. van Vliet,^{6,7} F. A. Bastiaan von Meijenfeldt,⁸ Stefan Bertilsson,⁴ Laura Villanueva,^{8,9} Irene Sánchez-Andrea,⁶ Erik Björn,¹⁰ Andrea G. Bravo,³ Lars-Eric Heimbürger Boavida¹

AUTHOR AFFILIATIONS See affiliation list on p. 15.

ABSTRACT In the global context of seawater deoxygenation triggered by climate change and anthropogenic activities, changes in redox gradients impacting biogeochemical transformations of pollutants, such as mercury, become more likely. Being the largest anoxic basin worldwide, with high concentrations of the potent neurotoxic methylmercury (MeHg), the Black Sea is an ideal natural laboratory to provide new insights about the link between dissolved oxygen concentration and *hgcAB* gene-carrying (*hgc*⁺) microorganisms involved in the formation of MeHg. We combined geochemical and microbial approaches to assess the effect of vertical redox gradients on abundance, diversity, and metabolic potential of *hgc*⁺ microorganisms in the Black Sea water column. The abundance of *hgcA* genes [congruently estimated by quantitative PCR (qPCR) and metagenomics] correlated with MeHg concentration, both maximal in the upper part of the anoxic water. Besides the predominant *Desulfobacteriales*, *hgc*⁺ microorganisms belonged to a unique assemblage of diverse—previously underappreciated—anaerobic fermenters from *Anaerolineales*, *Phycisphaerae* (characteristic of the anoxic and sulfidic zone), *Kiritimatiellales*, and *Bacteroidales* (characteristic of the suboxic zone). The metabolic versatility of *Desulfobacterota* differed from strict sulfate reduction in the anoxic water to reduction of various electron acceptors in the suboxic water. Linking microbial activity and contaminant concentration in environmental studies is rare due to the complexity of biological pathways. In this study, we disentangle the role of oxygen in shaping the distribution of Hg-methylating microorganisms consistently with MeHg concentration, and we highlight their taxonomic and metabolic niche partitioning across redox gradients, improving the prediction of the response of marine communities to the expansion of oxygen-deficient zones.

IMPORTANCE Methylmercury (MeHg) is a neurotoxin detected at high concentrations in certain marine ecosystems, posing a threat to human health. MeHg production is mainly mediated by *hgcAB* gene-carrying (*hgc*⁺) microorganisms. Oxygen is one of the main factors controlling Hg methylation; however, its effect on the diversity and ecology of *hgc*⁺ microorganisms remains unknown. Under the current context of seawater deoxygenation, mercury cycling is expected to be disturbed. Here, we show the strong effect of oxygen gradients on the distribution of potential Hg methylators. In addition, we show for the first time the significant contribution of a unique assemblage of potential fermenters from *Anaerolineales*, *Phycisphaerae*, and *Kiritimatiellales* to Hg methylation, stratified in different redox niches along the Black Sea gradient. Our results considerably expand the known taxonomic diversity and ecological niches prone to the formation of MeHg and contribute to better apprehend the consequences of oxygen depletion in seawater.

Editor Michael S. Rappe, University of Hawaii at Manoa, Kaneohe, Hawaii, USA

Address correspondence to Léa Cabrol, lea.cabrol@mio.osupytheas.fr, or Eric Capo, eric.capo@umu.se.

Léa Cabrol and Eric Capo are joint first authors. Order of names was decided based on involved contributions.

Andrea G. Bravo and Lars-Eric Heimbürger Boavida are co-last authors.

The authors declare no conflict of interest.

See the funding table on p. 15.

Received 24 May 2023

Accepted 16 June 2023

Published 14 August 2023

Copyright © 2023 Cabrol et al. This is an open-access article distributed under the terms of the [Creative Commons Attribution 4.0 International license](https://creativecommons.org/licenses/by/4.0/).

KEYWORDS mercury methylation, diversity, *hgcAB* gene, metagenomics, redoxcline, niche partitioning, qPCR, MAGs

Decades of anthropogenic emissions and widespread atmospheric dispersal make mercury (Hg) a contaminant of global concern (1). Hg can be transformed into the neurotoxin methylmercury (MeHg) and detected at high concentrations in certain marine ecosystems, where it bioaccumulates and biomagnifies, ultimately causing severe risks for humans (2). The methylation of Hg^{II} to MeHg is mainly mediated by microorganisms and has primarily been described in anoxic environments such as wetlands, sediments, rice paddies, or animal gut (3). Aside from the *sine qua non* presence and activity of microorganisms producing MeHg, Hg methylation is also controlled by Hg bioavailability, organic matter composition, and oxygen concentrations. Relatively high MeHg concentrations and Hg methylation potential have been reported in oxygen-deficient water columns (4, 5). However, there is still limited knowledge about the microbial key players involved in Hg methylation in marine ecosystems and the environmental conditions constraining their activity (6).

Microbial methylation of Hg has been shown to involve and rely on the enzyme coded by the gene pair *hgcA* and *hgcB* (7). Microorganisms that harbor these genes (*hgcAB* gene-carrying [*hgc*⁺] microorganisms), and the methylation capacity they provide, have been identified across diverse microbial lineages and different environments (8–10). Most cultivated lineages with experimentally validated Hg methylation capacity have been affiliated to sulfate-reducing, iron-reducing, and/or syntrophic-fermenting bacteria from *Desulfobacterota* and *Firmicutes*, as well as to methanogenic *Archaea* (3, 11, 12). Recent high-throughput sequencing analyses, including the reconstruction of metagenome-assembled genomes (MAGs) from environmental samples, have revealed a broader diversity of putative Hg methylators including previously unknown and largely uncultured *hgc*⁺ microorganisms such as *Planctomycetota*, *Verrucomicrobiota*, *Chloroflexota*, and *Nitrospirota* (13–16), some of them being found abundantly in coastal and “dead zone” systems, such as the fully anoxic bottom waters of a stratified fjord (10), a seasonally anoxic fjord (Saanich Inlet) (17), and oxygen-deficient brackish water from the Baltic Sea (18, 19). These studies corroborate that the main methylators differ between ecosystems and along dominant redox gradients.

In the ocean, climate change and human activities lead to current—and further expected—seawater deoxygenation and expansion of oxygen-deficient zones (20). The modification of redox gradients can dramatically affect microbial and biogeochemical cycles, including Hg transformations. Since the Black Sea is the largest and deepest permanently euxinic (anoxic and sulfidic conditions) stratified basin worldwide, with stable redox gradients extending over several tens of meters (21, 22), it is a promising target to study the partitioning of Hg-methylating microorganisms over contrasted redox niches. A stable permanent pycnocline prevents mixing and exchange between the upper oxygenated layers and anoxic deep waters, separated by a suboxic water layer extending from 75 to 120 m (down to 240 m at certain coastal stations) (23). In the Black Sea water column, high concentrations of MeHg concentrations have been reported in the suboxic and anoxic water layers (24, 25). The high horizontal (isopycnal) homogeneity of the Black Sea has been demonstrated, in terms of microbial community composition (26), hydrography (27), and geochemistry, including Hg chemistry (25). However, the microorganisms involved in Hg methylation in the Black Sea water column have not been identified yet, neither the effect of the vertical stratification on their composition. As reported for other euxinic systems (e.g., Baltic Sea, Cariaco Basin, Saanich Inlet), it is plausible that the vertical gradient of oxygen and HS⁻ concentrations in the Black Sea shapes the distribution of microbial communities, including those involved in MeHg formation, as well as their associated metabolic and biogeochemical functions (22, 28–30).

In this study, we aimed to determine the impact of the vertical redox gradient on the microorganisms potentially responsible for Hg methylation in the water column of the Black Sea. We combined geochemical and molecular data obtained from two sampling campaigns conducted in 2013 that had resulted in the previous characterization of (i) high-resolution Hg and MeHg concentrations throughout full water column transects (25) and (ii) specific (sulfur- and organic matter-linked) microbial metabolisms through genome-centric metagenomics (29–31). We used several molecular analyses including 16S rRNA amplicon sequencing, metagenomics, and clade-specific quantitative PCR of the *hgcA* gene, at different depths, to determine whether the highest concentrations of MeHg observed in the anoxic water layers of the Black Sea were explained by the presence, abundance, and metabolic traits of *hgc*⁺ microorganisms. The present study is novel in revealing the oxygen-dependent niche partitioning of diverse microorganisms potentially capable of Hg methylation in the Black Sea, consistently with measured MeHg concentrations.

MATERIALS AND METHODS

Sampling campaigns

Two complementary field cruises were conducted almost simultaneously in June–July 2013 in the Black Sea with the vessel R/V Pelagia to obtain (i) Hg chemistry data, *hgcA* quantitative PCR (qPCR), and 16S rRNA gene amplicon sequencing data (MEDBlack cruise) and (ii) planktonic metagenomes (Phoxy cruise). Following the definitions in Stewart et al. (32) and the vertical discretization model of Rosati et al. (25), the water column was decomposed into three redox layers: the oxic layer (OL, from 0 to 75 m depth, characterized by O₂ concentrations between 30 and 300 μM and undetectable HS[−] concentrations), the suboxic layer (SOL, from 75 to 120 m depth, characterized by dissolved O₂ concentrations <20 μM and HS[−] concentrations <5 μM), and the anoxic layer (AOL, below 120 m depth, characterized by undetectable O₂ concentrations and HS[−] concentrations between 15 and 400 μM).

The MEDBlack cruise was conducted from 13 to 25 July 2013 and occupied 12 stations along a west-to-east transect. In the present work, we include five stations (1, 2, 5, 6, and 9, according to previous nomenclature [25]; Fig. 1). For microbiology, water samples were collected from three water depths: OL (30–50 m), SOL (90–110 m, except coastal station 6 sampled at 180 m depth), and AOL (140–150 m, except coastal station 6 sampled at 250 m depth) (exact sampling depths are provided in Data Sheet S1A). Samples were filtered with *in situ* Stand Alone Pump System (Challenger Oceanic, from NOC, Southampton) equipped with two 293 mm diameter filters: a Petex nylon mesh pre-filter (51 μm; 150 μm for station 1) and a polycarbonate filter (1 μm) further stored at −20°C.

The Phoxy cruise 64PE371 was conducted on 9 and 10 June 2013 in the western gyre of the Black Sea. Suspended particulate matter was collected from 15 depths across the oxygen gradient in the water column (from 50 to 2,000 m depth) at sampling station 2 (42.89 N, 30.67 E, 2,107 m depth [Fig. 1], at 72 km from the MEDBlack station 2 and visited 35 days earlier) with McLane WTS-LV *in situ* pumps (McLane Laboratories Inc., Falmouth, MA, USA) on pre-combusted glass fiber filters with 142 mm diameter and 0.7 μm nominal pore size, further stored at −80°C. One sample from the Phoxy cruise belonged to the OL (50 m depth), eight samples to the SOL (70–110 m depth), and six samples to the AOL (130–2000 m depth).

Physicochemical measurements

For the Phoxy cruise, chemical parameters included the dissolved concentrations of O₂, HS[−], NH₄⁺, NO₂[−], and NO₃[−] (Data Sheet S1B). Dissolved O₂ concentration was measured by a conductivity-temperature-depth (CTD) probe equipped with a Seabird SBE 43 electrochemical O₂ sensor which was calibrated against on-deck Winkler titrations, with a detection limit of 2 μM. Nutrients concentrations were measured on a QuAatro

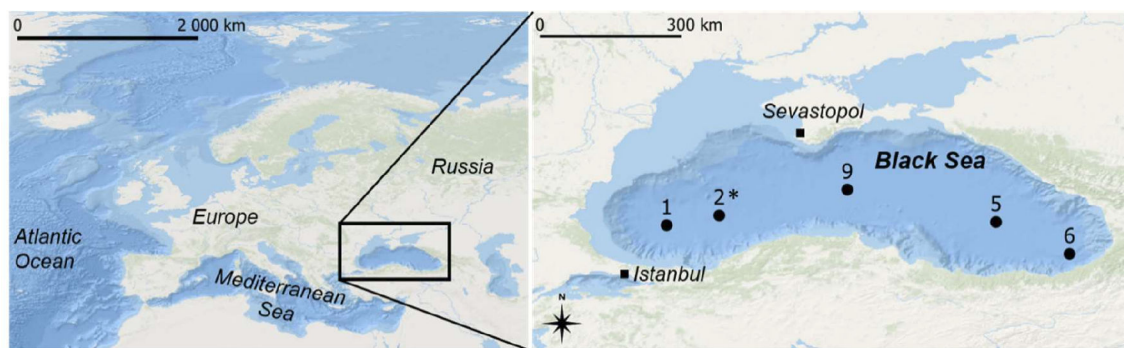


FIG 1 Locations of stations sampled in the Black Sea during the MEDBlack cruise and analyzed in this study (black dots). The star indicates station 2 which was also sampled during the Phoxy cruise for metagenomics analysis. The exact coordinates are provided in Data Sheet S1A.

autoanalyzer with a detection limit of 0.26, 0.031, 0.011, 0.007, and 0.008 μM for HS^- , NH_4^+ , NO_3^- , NO_2^- , and PO_4^{3-} , respectively (33). A summary of available and new data for both campaigns is provided in Table 1.

TABLE 1 Description of samples included in this study and summary of the main measured geochemical parameters, available from Rosati et al. (25) (for MEDBlack samples) and from Sollai et al. (33) (for Phoxy cruise)^a

| Sample name | Cruise campaign | Sampling depth (m) | Concentrations of dissolved elements | | | | | | Method |
|-------------|-----------------|--------------------|--------------------------------------|---------------------------------|-----------------------------------|--------------------------------------|----------|-----------|----------|
| | | | O_2 (μM) | HS^- (μM) | NH_4^+ (μM) | PO_4^{3-} (μM) | tHg (pM) | MeHg (pM) | |
| F1-OL | MEDBlack | 55.5 | 142.4 | <LoD | <LoD | 0.7 | 1.4 | 0.2 | MB, qPCR |
| F1-SOL | MEDBlack | 85.7 | 3.4 | <LoD | 0.1 | 0.9 | 1.4 | 0.1 | MB, qPCR |
| F1-AOL | MEDBlack | 145.3 | <LoD | 19.3 | 13.5 | 5.0 | 3.1 | 0.8 | MB, qPCR |
| F2-OL | MEDBlack | 24.2 | 423.0 | <LoD | 0.2 | <LoD | 3.3 | 0.1 | MB, qPCR |
| F2-SOL | MEDBlack | 99.5 | 1.8 | <LoD | 3.9 | 6.2 | 1.6 | 0.2 | MB, qPCR |
| F2-AOL | MEDBlack | 144.8 | <LoD | 22.6 | 15.2 | 5.0 | 5.3 | 0.8 | MB, qPCR |
| F9-OL | MEDBlack | 45.8 | 213.1 | <LoD | 0.1 | 0.8 | 2.2 | 0.1 | MB, qPCR |
| F9-SOL | MEDBlack | 100.4 | 1.8 | <LoD | 2.0 | 6.6 | 2.2 | 0.2 | MB, qPCR |
| F9-AOL | MEDBlack | 149.6 | <LoD | 17.7 | 15.8 | 4.8 | 3.6 | 1.1 | MB, qPCR |
| F5-OL | MEDBlack | 40.5 | 373.8 | <LoD | 0.1 | <LoD | 2.8 | 0.1 | MB, qPCR |
| F5-SOL | MEDBlack | 110.4 | 1.8 | <LoD | 3.6 | 7.0 | 3.2 | 0.4 | MB, qPCR |
| F5-AOL | MEDBlack | 149.4 | <LoD | 15.3 | 13.8 | 4.8 | 3.3 | 0.8 | MB, qPCR |
| F6-OL | MEDBlack | 40.3 | 377.0 | <LoD | <LoD | <LoD | 3.0 | 0.1 | MB, qPCR |
| F6-SOL | MEDBlack | 175.0 | 10.7 | <LoD | 0.2 | 3.1 | 2.9 | 0.4 | MB, qPCR |
| F6-AOL | MEDBlack | 250.3 | <LoD | 36.5 | 19.2 | 4.9 | 3.3 | 0.8 | MB, qPCR |
| F2-50 | Phoxy | 50 | 121.2 | <LoD | 0.1 | 0.7 | Nd | Nd | MG |
| F2-70 | Phoxy | 70 | 2.2 | <LoD | 0.1 | 1.1 | Nd | Nd | MG |
| F2-80 | Phoxy | 80 | <LoD | <LoD | 0.1 | 1.1 | Nd | Nd | MG |
| F2-85 | Phoxy | 85 | <LoD | <LoD | 0.1 | 0.8 | Nd | Nd | MG |
| F2-90 | Phoxy | 90 | <LoD | <LoD | 0.4 | 2.1 | Nd | Nd | MG |
| F2-95 | Phoxy | 95 | <LoD | <LoD | 1.1 | 4.7 | Nd | Nd | MG |
| F2-100 | Phoxy | 100 | <LoD | <LoD | 5.7 | 7.2 | Nd | Nd | MG |
| F2-105 | Phoxy | 105 | <LoD | 0.9 | 7.2 | 7.9 | Nd | Nd | MG |
| F2-110 | Phoxy | 110 | <LoD | 4.6 | 8.8 | 6.7 | Nd | Nd | MG |
| F2-130 | Phoxy | 130 | <LoD | 14.7 | 13.9 | 5.5 | Nd | Nd | MG |
| F2-170 | Phoxy | 170 | <LoD | 31.6 | 20.1 | 4.9 | Nd | Nd | MG |
| F2-250 | Phoxy | 250 | <LoD | 84.7 | 32.6 | 5.2 | Nd | Nd | MG |
| F2-500 | Phoxy | 500 | <LoD | 206.3 | 59.8 | 6.8 | Nd | Nd | MG |
| F2-1000 | Phoxy | 1,000 | <LoD | 353.8 | 90.8 | 7.9 | Nd | Nd | MG |
| F2-2000 | Phoxy | 2,000 | <LoD | 397 | 100.2 | 8.4 | Nd | Nd | MG |

^aDetailed data sets including additional measured parameters are provided in Data Sheet S1A and B. Nd, non-determined; LoD, limit of detection. The “method” column stands for the molecular methods applied in the current study: MB for metabarcoding, qPCR for quantitative PCR, MG for metagenomics.

For the MEDBlack cruise, available measured physicochemical parameters (Data Sheet S1A) include pressure, temperature, conductivity, fluorescence, salinity, density, and the dissolved concentrations of O₂, HS⁻, NH₄⁺, NO₂⁻, NO₃⁻, PO₄³⁻, Si, Fe, DOC, total Hg, and MeHg (sum of mono- and di-MeHg) according to previous protocols (25). Specific analysis of Hg and MeHg is detailed in Supplemental Information 1.1. The detection limit was 0.025 and 0.001 pM for HgD and MeHgD, respectively. Nutrients, HS⁻, and dissolved O₂ concentrations were measured similarly to the Phoxy cruise with the same detection limits. Despite coming from two different cruises, the variability between nutrients, HS⁻, and dissolved O₂ concentrations measured in both cruises at similar depths is low (4–14% variability on average).

DNA extractions

From the MEDBlack cruise, DNA was extracted from sections of the 15 filters (i.e., five stations, three depths) with the FastDNA kit and FastPrep homogenizer (MP Biomedicals, Santa Ana, CA, USA) according to the manufacturer instructions. The filter fraction represented 2.5% of the whole filter area, corresponding to approximately 5–13 L of filtered seawater depending on the sampling points (8 L on average). From the Phoxy cruise, DNA was extracted from sections of 15 glass fiber filters (1/8 filter from 50 to 130 m depth and 1/4 from 170 to 2,000 m depth) with the RNA PowerSoil Total Isolation Kit plus the DNA elution accessory (Mo Bio Laboratories, Carlsbad, CA, USA) as previously described (31).

Amplicon sequencing and qPCR estimates of 16S rRNA genes

For the MEDBlack cruise DNA samples, the hypervariable V4-V5 region of the 16S rRNA gene from *Bacteria* and *Archaea* was amplified with high-fidelity Phusion Hot Start II DNA polymerase (Thermo Scientific, Waltham, MA, USA) using universal primers 515F and 928R (34) and a two-step PCR protocol (35), as detailed in Supplemental Information 1.2. and Table S1. The correct amplicon size and the absence of non-specific bands were checked by agarose gel electrophoresis. Amplicons were sequenced using a 2 × 250 bp paired-end MiSeq system (Illumina, USA) at the Genotoul platform (Toulouse, France). The raw sequences have been deposited at NCBI GenBank, SRA database, under the BioProject accession number [PRJNA895066](https://www.ncbi.nlm.nih.gov/bioproject/PRJNA895066).

Raw sequences were analyzed on the Galaxy bioinformatics platform through the FROGS pipeline, version 3.2.3, as detailed in the Supplemental Information. Especially, operational taxonomic units (OTUs) were defined by sequence clustering, using the high-resolution SWARM algorithm v3.2.3 (36). After filtering at 0.005% of abundance, OTUs were taxonomically annotated with the SILVA 16S database (version 138.1).

Bacterial and archaeal abundances were quantified in the MEDBlack cruise DNA samples by quantitative PCR with Takyon No Rox SYBR 2X Master Mix (Eurogentec, Seraing, Belgium). Protocol details are provided in Table S1.

Clade-specific *hgcA* gene qPCR estimates and cloning sequencing of *hgcA* sequences

In the MEDBlack cruise DNA samples, the *hgcA* genes of each of the three dominant Hg-methylating clades (*Desulfobacterota*, *Firmicutes*, and *Archaea*) were quantified by qPCR, using clade-specific degenerated qPCR primers (37) and Takyon No Rox SYBR 2X Master Mix (Eurogentec, Seraing, Belgium). The qPCR conditions have been optimized as detailed in the Supplemental Information. All qPCR details and primer sequences are provided in Supplemental Information 1.3. and Table S1.

For *Archaea-hgcA*, due to the low amplification efficiency and the ambiguity in the melting curves and agarose gel electrophoresis, the correct affiliation of the *hgcA* amplicons was verified by cloning and sequencing the amplified PCR product, as detailed in Supplemental Information 1.4. Obtained DNA sequences were translated into amino acid sequences and compared with *hgcA* sequences from the Hg-MATE database

(38) and from the 15 metagenomes obtained in the Phoxy cruise (see following section). The sequence analysis (Supplemental Information 1.4 and Fig. S2) showed that *hgcA* sequences obtained with this primer set clustered with *Euryarchaeota* and *Chloroflexota* sequences. Thus, from thereon, *hgcA* qPCR estimates from *Archaea* will be referred to *hgcA* qPCR estimates from *Archaea-Chloroflexota*.

Metagenomic estimates of *hgcA* genes

The 15 DNA extracts from the Phoxy cruise were used to prepare TruSeq nano libraries, sequenced with Illumina MiSeq (five samples multiplexed per lane) at Utrecht Sequencing Facility, generating 4.5×10^7 paired-end reads (2×250 bp), which were further processed as previously reported (31) and summarized in Supplemental Information 1.5.

hgc homologs were identified and annotated in the amino acid FASTA file (generated from protein-coding genes detected in the metagenomes coassembly), using the HMM profiles of *hgcA* and *hgcB* genes derived from the Hg-MATE database v1.01142021 (38) and the function *hmmsearch* from HMMER 3.2.1 (39). We considered genes with *E*-values $<10^{-3}$ as significant hits. To further confirm putative *hgcA* and *hgcB* genes (or *hgc*-like genes) within the HMM search hits, we used the high stringency cutoff defined by Capo et al. (8) by looking for unique conserved motifs from *hgcA* gene (NVWCA(A/G/S)GK) and performed a manual inspection of the presence of *hgcA* genes. Coverage values of *hgcA* genes were calculated as the number of reads mapped to the gene divided by its length (base pairs, bp) and were further normalized by dividing them by the coverage values of the marker gene *rpoB*. The *rpoB* genes were detected using the function *hmmsearch* from HMMER 3.2.1 (39) and HMM profile TIGR02013.hmm for bacterial *rpoB* genes and applying the trusted cutoff provided in HMM files.

The obtained *hgcA* homologs, translated in amino acid sequences, were taxonomically affiliated through a phylogenetic analysis, by placing them onto the HgcA reference tree using a *pplacer* approach (40). The construction of the reference tree was based on the reference package "hgcA" from Hg-MATE database v1, according to the protocol in the README.txt of the Hg-MATE database (38) and in Capo et al. (8), as detailed in Supplemental Information 1.5. As a complement to this community-level analysis, metagenome-assembled genomes generated from the same previously published metagenomes (30, 31) were screened for *hgc* genes. The *hgc* genes found in MAGs were taxonomically identified using the MAG phylogeny and taxonomy (Data Sheet S1D).

Data analysis

The qPCR estimates were statistically analyzed by two-way analysis of variance (ANOVA) with the *aov* function (R software). The selected environmental parameters for correlation analysis were the concentrations of dissolved O_2 , HS^- , and MeHg. Spearman correlation plots were obtained using the functions *rcorr* and *corrplot* from the R packages *Hmisc* and *corrplot*, respectively. Shannon diversity indices were calculated with the *estimate_richness* function in the *vegan* R package. Principal coordinates analysis (PCoA) was performed applying the function *wcmdscale* to Bray-Curtis dissimilarity matrixes built with the function *vegdist* from the 16S rRNA gene-based OTU abundance table and the *hgcA* gene abundance (normalized coverage values) in the R package *vegan*. The discriminant *hgcA* genes explaining the most the clustering of *hgc*⁺ community according to depth zones were identified by linear discriminant analysis (*run_lefse* function, *microbiomeMarker* package) with cumulative sum scaling normalization and 100 bootstraps.

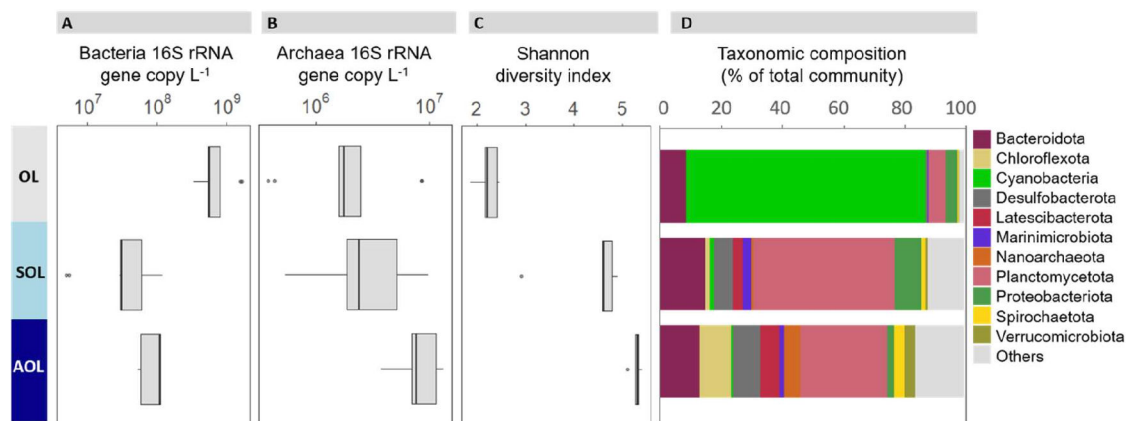


FIG 2 Stratification of microbial profiles in the Black Sea water column. Data from the five sampling stations have been averaged for oxic (OL, 25–50 m), suboxic (SOL, 85–110 m, except station 6 at 175 m), and anoxic (AOL, 145–250 m) layers. (A) qPCR quantification of bacterial 16S rRNA gene, per filtered volume of seawater. (B) qPCR quantification of archaeal 16S rRNA gene, per filtered volume of seawater. (C) Diversity of total microbial community based on Shannon index, computed from 16S rRNA gene amplicon sequences. (D) Taxonomic composition of microbial communities at the phylum level, representing the 11 most abundant phyla. In panels A to C, the bold line of each boxplot shows the median, while upper and lower limits of the boxes represent the first and third quartiles, respectively. The whiskers are maximum and minimum values and the dots show the outliers. For panel D, for each phylum, the averages and standard deviations calculated per water layer are provided in Data Sheet S1E. The taxonomic composition of the five individual sampling stations across the Black Sea basin is shown in Fig. S3 (at the phylum level) and the detailed OTU composition is provided in Data Sheet S1C.

RESULTS

Mercury and microbial community stratification along water depth and oxygen gradient

Hg and MeHg profiles revealed a strong depth stratification, homogeneous across the whole basin (Fig. S1). In stations 1, 2, and 5, the MeHg concentration was always maximal at the same depth (130 m) reaching 0.83–1.13 pM, which represents 32%–48% of tHg at this depth. The MeHg concentration then decreased down to 250 m depth and remained relatively stable in deeper waters (0.50–0.65 pM on average below 250 m depth, representing 19%–26% of tHg).

Microbial community structure was homogeneous horizontally across the Black Sea basin, but vertically stratified across water depth and oxygen concentrations. Considering the MEDBlack samples, bacterial abundances based on qPCR of the bacterial 16S rRNA gene did not significantly differ along the west-to-east transect (two-way ANOVA, $P = 0.4$) but were significantly impacted by sampling depth (two-way ANOVA, $P < 0.001$) (Fig. 2A; Data Sheet S1A). The highest bacterial abundances (7.8×10^8 16S copies L^{-1} on average) were observed in the OL (30–50 m depth), being one order of magnitude higher than in the AOL (140–250 m depth). Archaeal abundances measured by qPCR also varied with depth ($P = 0.001$), but showed a reverse stratification pattern from bacteria (Fig. 2B) as detailed in Supplemental Information 2.1.

The taxonomic composition (Fig. S3) and the structure (Fig. 3A) of the prokaryotic community was similar across the west-east transect, as confirmed by the non-significant effect of sampling station on the community structure permutational multivariate analysis of variance (PERMANOVA $P > 0.1$) and Shannon diversity (ANOVA, $P = 0.16$). For all stations, OL communities were dominated by *Cyanobacteria* representing 70% of prokaryotes (Fig. 2D; Fig. S3; Data Sheet S1C and E). SOL and AOL were significantly more diverse (ANOVA, $P < 0.001$, Fig. 2C), dominated by *Planctomycetota* (29%–47% of the prokaryotes), *Bacteroidota* (13%–15%), and *Desulfobacterota* (7%–9%) (Supplemental Information 2.1).

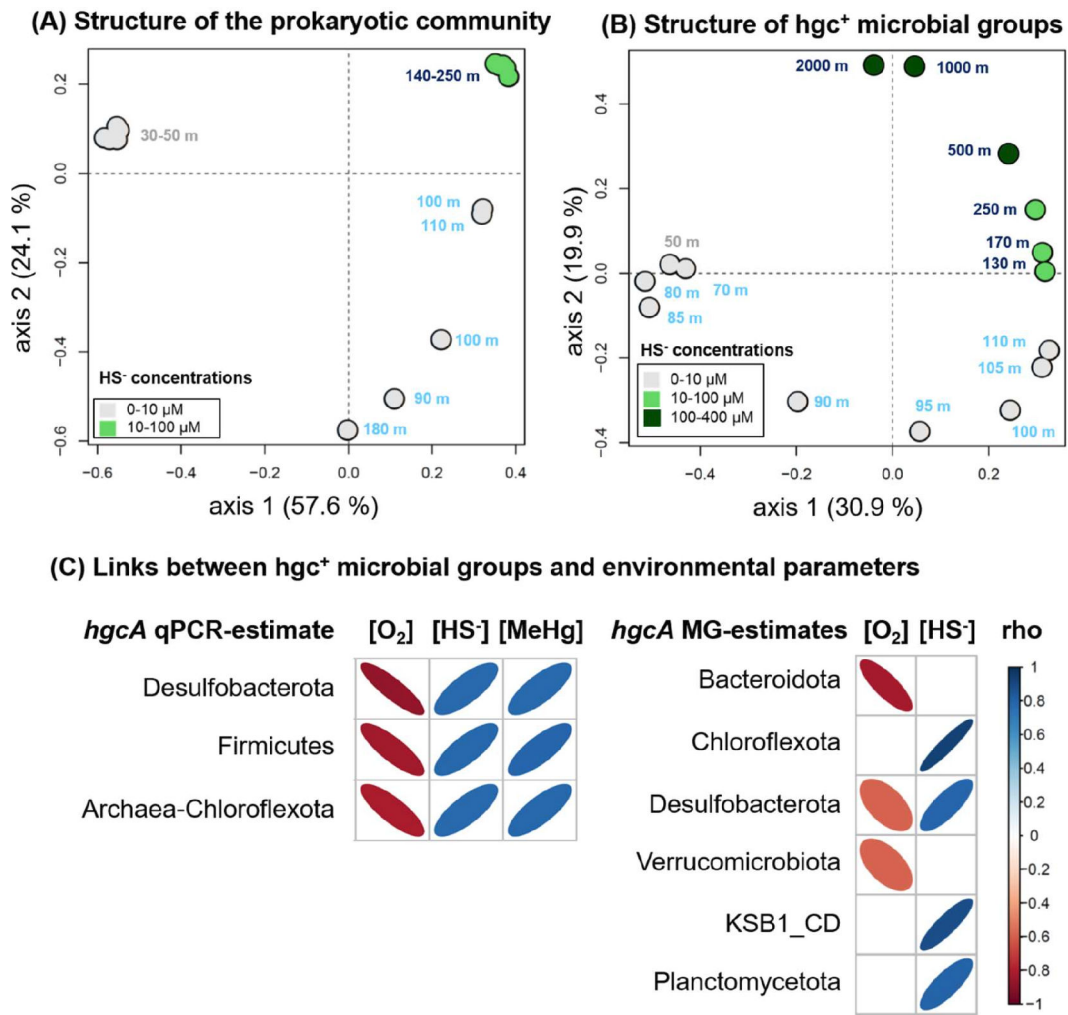


FIG 3 Depth stratification of prokaryotic and *hgc*⁺ communities in relation with environmental gradients and Hg-related variables. (A and B) PCoA plots based on Bray-Curtis dissimilarity showing the structure of the overall prokaryotic community (A; MEDBlack cruise samples) and of the *hgc*⁺ microbial groups (B; Phoxy cruise samples). The dot color denotes the HS⁻ concentrations measured in the same samples. The color of the sample name label corresponds to the three water-depth zones: the oxic (OL, gray), suboxic (SOL, light blue), and anoxic (AOL, dark blue) water layers. (C) Correlation plots based on Spearman correlation coefficients between environmental parameters (O₂, HS⁻, and MeHg concentrations) and qPCR and metagenomic (MG) estimates of *hgcA* genes from different microbial groups. Only significant relationships (*P* < 0.05) are displayed. No MeHg measurements were done during the Phoxy cruise (metagenome samples).

Clade-specific *hgcA* genes measured by qPCR are more abundant in the anoxic layer

Abundance of *hgcA* genes was quantified by qPCR for each of the well-known Hg-methylating clades *Desulfobacterota*, *Firmicutes*, and *Archaea-Chloroflexota* (37) (see Supplemental Information 1.4 for the clade definition). Analogous to 16S rRNA gene counts, absolute *hgcA* counts from *Desulfobacterota*, *Firmicutes*, and *Archaea-Chloroflexota* were similar along the west-to-east transect of the Black Sea (two-way ANOVA, *P* > 0.90), but strongly stratified over depth (two-way ANOVA, *P* < 0.0001). Tracking the MeHg concentration profiles (Fig. 4A; Fig. S1), the highest *hgcA* counts were found in the AOL for all three clades, reaching on average $9.0 \pm 3.0 \cdot 10^3$, $6.1 \pm 1.4 \cdot 10^6$, and $5.6 \pm 1.5 \cdot 10^6$ copies L⁻¹ of seawater for *Firmicutes*, *Desulfobacterota*, and *Archaea-Chloroflexota*, respectively (Fig. 4B; Data Sheet S1A). The *hgcA* counts were between 12 and 31 times lower in the OL. In the SOL and AOL, *hgcA* counts from *Desulfobacterota* and *Archaea-Chloroflexota* were similar, exceeding that of *Firmicutes* by one to three orders of magnitude.

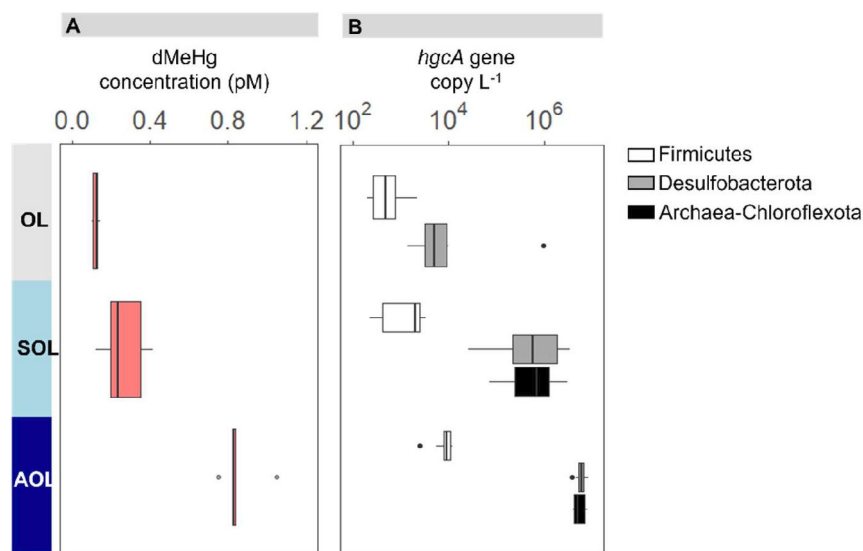


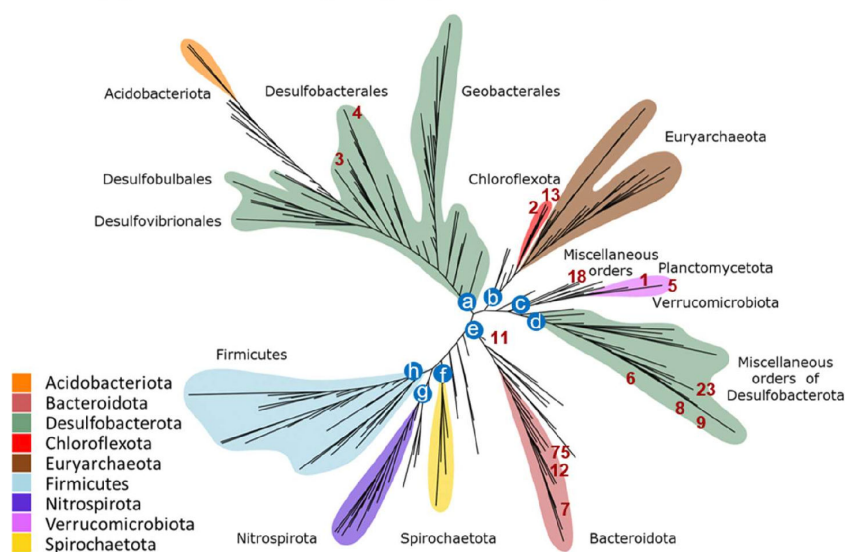
FIG 4 Vertical stratification of MeHg concentrations and *hgcA* gene abundances in the Black Sea water column. Data from the five sampling stations have been averaged for oxic (OL, 25–50 m), suboxic (SOL, 85–110 m, except station 6 at 175 m), and anoxic (AOL, 145–250 m) layers. (A) Dissolved concentration of MeHg. (B) qPCR quantification of *hgcA* gene, indicator of Hg methylation ability, for *Firmicutes*, *Desulfobacterota*, and *Archaea-Chloroflexota*, in copies per seawater filtered volume. The bold line of each boxplot shows the median, while upper and lower limits of the boxes represent the first and third quartiles, respectively. The whiskers are maximum and minimum values and the dots show the outliers. The values for the five individual sampling stations are provided in Data Sheet S1A, as well as the relative *hgcA* counts (normalized by total prokaryotic abundance).

The higher abundance of *hgcA* genes in the AOL was not only observed for absolute *hgcA* counts, but also for relative *hgcA* counts (normalized by summed bacterial and archaeal 16S gene counts, Data Sheet S1A), which contrasts with the pattern observed for total bacteria and indicates a clear enrichment of potential Hg methylators in oxygen-deficient deeper waters. Relative *hgcA* counts from *Desulfobacterota* represented 4.8%–9.8% of the prokaryotes in the AOL, 0.5%–2.9% in the SOL, and <0.2% in the OL. *hgcA* counts from *Archaea-Chloroflexota* followed a similar depth pattern, representing 4.3%–6.9% of the prokaryotes in the AOL and 0.8%–2% in the SOL, while not detected in the OL. Finally, *Firmicutes-hgcA* genes accounted for <0.02% of the prokaryotes in all layers. The specificity of the *Archaea-Chloroflexota hgcA* primers is further evaluated and discussed in the Supplemental Information.

hgc genes in the water column are affiliated to diverse taxa with specific niches

A total of 91 *hgcA* genes were found in the Black Sea metagenome co-assembly, including 14 genes found next to *hgcB* genes on the same contig (Data Sheet S1D). Among them, 15 *hgcA* genes were found in MAGs affiliated to various orders of *Desulfobacterota* (*Desulfobacterales*, *Desulfobulbales*, unclassified), *Chloroflexota* (*Anaerolineales*), *Bacteroidota* (*Bacteroidales*), *Planctomycetota* (*Phycisphaerales*), *Verrucomicrobiota* (*Kiritimatiellales*), and KSB1 candidate division (unclassified) (Fig. 5A). Among *Desulfobacterota*, the *hgc*⁺ MAGs were identified as uncultured species of *^UDesulfacyla*, *^UDesufatibia*, *^UDesulfobia*, and *Desulfobacula*. From the alignment to the Hg-MATE database, the remaining 76 unbinned *hgcA* genes were affiliated predominantly to *Desulfobacterota* (32), *Planctomycetota* (14, among which 4 *Phycisphaerae*), *Verrucomicrobiota* (9 *Kiritimatiellales*), *Chloroflexota* (8 *Anaerolineales*), and various microbial lineages (Data Sheet S1D).

(A) Taxonomic diversity of *hgcA* genes from metagenomes



(B) Vertical distribution of *hgcA* genes from metagenomes

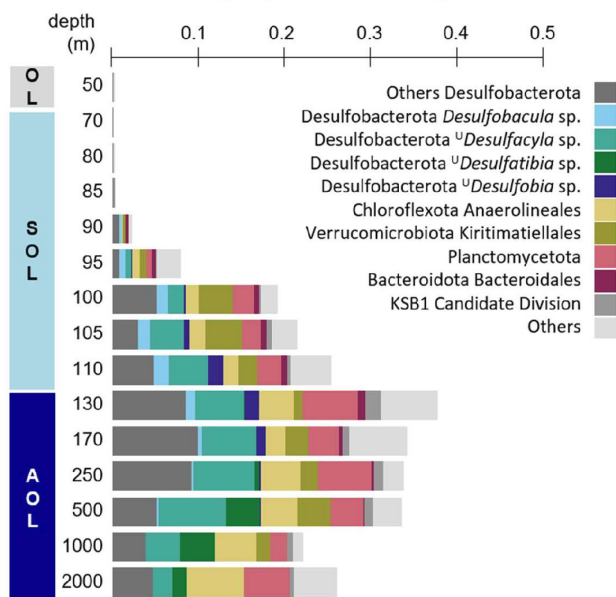


FIG 5 A diverse microbial community potentially able to methylate Hg in the Black Sea water column. (A) Unrooted *hgcA* phylogenetic tree showing the diversity of *hgcA*⁺ microorganisms from the Black Sea water column compared to the reference sequences from the Hg-MATE database. The 15 binned *hgcA* genes found in MAGS are denoted in the figure by their ID number in red (see “gene_id” in Data Sheet S1D). The other 77 unbinned *hgcA* genes are listed in Data Sheet S1D; after examination of their placement on the phylogenetic tree, they were assigned to a taxonomic cluster denoted from “a” to “h” (indicated in the column “Corresponding cluster in *hgcA* tree” of Data Sheet S1D). For clarity purpose, only the cluster letter is shown on the tree (blue circles at the basis of each group) instead of the 77 sequences. The reference phylogenetic tree was provided by the Hg-MATE database using *hgcA* sequences from (i) pure culture/environmental microbial isolates (204 sequences), (ii) single-cell genome sequences (29 sequences), and (iii) metagenome-assembled genomes (787 sequences), as detailed in Materials and Methods and Supplemental Information 1.5. (B) Vertical distribution of MG-estimated coverage values of *hgcA* genes normalized by *rpoB* coverage values along the water column depth in the Black Sea. The corresponding compartmentation into oxic (OL), suboxic (SOL), and anoxic (AOL) layers is shown on the left axis. Color code corresponds to taxonomic affiliation.

The metagenome-estimated (MG-estimated) abundance and diversity of *hgcA* genes were both strongly stratified along the Black Sea water column (Fig. 5B; Data Sheet S1B). This was in line with the qPCR results for clade-specific *hgcA* genes, although samples for metagenomic analysis were collected with a higher vertical resolution (15 depths). *hgcA* genes were barely detected in the OL and at the top of the SOL (<0.1% of the reads above 70 m depth). The abundance of *hgcA* genes (i.e., normalized coverage values) gradually increased over depth, reaching the highest value at the SOL-AOL transition (130 m depth, 14.3% of the total *hgcA* abundance). In deeper water layers, *hgcA* abundance decreased to 8.4%–9.9% at 1,000–2,000 m depth. MG-derived *hgcA* genes from *Desulfobacterota* were predominant in both the SOL (28.3%–58.4% of all *hgcA* genes) and the AOL (33.0%–53.8%). The second most abundant MG-derived *hgcA* sequences belonged to *Anaerolineales* and *Phycisphaerae* and predominated in the AOL (representing, respectively, $15.1 \pm 6.8\%$ and $6.4 \pm 3.1\%$ of all *hgcA* in this layer), while *hgcA* genes from *Kiritimatiellales* and *Bacteroidales* predominated in the SOL ($12.9 \pm 10.1\%$ and $5.9 \pm 5.5\%$, respectively). At 1,000 and 2,000 m depths, where HS^- concentrations were the highest (>350 μM), the proportion of *hgcA* genes from *Verrucomicrobiota* and $^{\text{U}}\text{Desulfacyla}$ decreased, while those from other *Desulfobacterota* and *Chloroflexota* remained dominant (Fig. 5B; Data Sheet S1B). Also, *hgcA* genes from *Firmicutes* represented 1.4%–6.7% of all reads at the SOL-AOL transition (110–130 m), while they were undetected in all the other sampled depths (Data Sheet S1B and D).

Relationships between environmental gradients, Hg-related variables, and microbial stratification over depth

PCoA analyses showed that the structure of both the 16S rRNA gene-based prokaryotic community (Fig. 3A) and *hgc*⁺ microbial groups (Fig. 3B) clustered similarly with depth (PERMANOVA, $P < 0.05$), according to the three redox zones (OL, SOL, and AOL). This microbial stratification over depth can be related to the observed geochemical gradients of oxygen, HS^- , and MeHg concentrations, along with other stratified parameters (Table 1).

For the MEDBlack samples, the qPCR-estimated abundances of *hgcA* genes from *Desulfobacterota*, *Firmicutes*, and *Archaea-Chloroflexota* were significantly positively correlated with MeHg and HS^- concentrations, and negatively correlated with oxygen concentrations (Spearman rank correlations, P -value <0.01; Fig. 3C). Several other environmental parameters also appeared to be stratified and co-varied with oxygen along depth (Table 1).

For station 2 studied in the Phoxy cruise, the correlations between the MG-estimated abundance of *hgcA* genes and environmental conditions depended on the microbial groups (Fig. 3C). The abundances of *hgcA* genes from *Bacteroidota* and *Verrucomicrobiota* significantly increased with oxygen depletion but were not significantly correlated to HS^- concentrations. In contrast, *hgc*⁺ *Chloroflexota*, KSB1 Candidate Division, and *Planctomycetota* were positively correlated to HS^- concentrations and not significantly related to oxygen concentrations. Finally, *hgcA* genes from *Desulfobacterota* were negatively correlated to oxygen concentrations and positively correlated to HS^- concentrations (Fig. 3C). The *hgc*⁺ community clustering in the AOL was characterized by discriminant *hgcA* genes affiliated to *Desulfobacterota* ($^{\text{U}}\text{Desulfatibia}$), *Chloroflexota* (*Anaerolineales*), and *Planctomycetota* (mainly from *Phycisphaerae*), while the *hgc*⁺ community in the SOL was discriminated by *hgcA* genes affiliated to *Kiritimatiellales*, $^{\text{U}}\text{Desulfacyla}$, *Bacteroidales*, *Desulfobacterales*, and other PVC (*Planctomycetota*, *Verrucomicrobiota*, and *Chlamydia*) superphylum members (Iefse analysis, $P < 0.05$, Fig. S4), thus confirming the oxygen-dependent niche partitioning of potential methylators at a fine taxonomic resolution.

DISCUSSION

Coupling methodological approaches to identify bioindicators of Hg methylation in the environment

Our 16S rRNA gene metabarcoding data support previous studies that reported the enrichment of *Desulfobacterota*, *Planctomycetota*, *Acidobacteriota*, and *Firmicutes* with increasing depth, and the restriction of *Nitrospirota*, *Chloroflexota*, and *Verrucomicrobiota* to the anoxic waters of the Black Sea (28, 41). Several of the dominant microbial lineages found in and below the redoxcline include *hgc*⁺ microorganisms. However, studies based on 16S rRNA gene taxonomic classification are often not sufficient to predict the occurrence of Hg methylators, since Hg methylation is a species- (and possibly strain-) specific trait (3). Alternative approaches targeting the *hgc* genes as a biomarker of microbial Hg methylation have been proposed (37, 42, 43). To avoid the biases due to the large polyphyletic diversity of the *hgcA* gene (9), and the overrepresentation of *hgcA* sequences from *Desulfobacterota* in databases of known Hg methylators used for primer design (8, 43), clade-specific qPCR primers have been developed, targeting *hgcA* genes from each of the three dominant Hg-methylating clades, i.e., *Desulfobacterota*, *Archaea*, and *Firmicutes* (37). This approach yielded results similar to metagenome-derived estimates for the identification of Hg methylation biomarkers (42), and is preferable to detect taxa-dependent correlations with environmental and/or functional outcomes. It is important to highlight that the outcomes of different methods should be interpreted cautiously since some discrepancies have been previously reported between, e.g., metagenomics, functional gene sequencing, cloning, qPCR, and 16S metabarcoding (14, 42, 44). Finally, DNA-based approaches should be complemented by gene expression and methylation rates measurements in order to confirm the involvement of potential Hg methylators.

Geochemical and microbial homogeneity along the Black Sea transect

Here, although qPCR and metagenomic estimates have been applied to samples from two different cruises, the results of the two cruises yield comparable results, including (i) similar stratification pattern of *hgcA* abundance across water depth and environmental conditions, and (ii) similar taxonomic identification and abundance distribution of putative Hg methylators. Even if metagenomic analysis has been carried out only at station 2 during the Phoxy cruise, our results are likely representative for the basin as a whole because of the high horizontal homogeneity of the Black Sea (excluding coastal areas), in terms of microbial community structure (as shown in the present and previous studies) (26) hydrography (27) and geochemistry (25). Here, all the microbial indicators and metrics (i.e., total abundances, abundance of *hgcA*-carriers from different clades, alpha diversity, community structure, and composition) were similar across the east-west transect, as well as the full-depth high-resolution Hg and MeHg concentration profiles. Significant positive correlations were observed between *hgcA* qPCR estimates from the three targeted microbial groups (i.e., *Desulfobacterota*, *Firmicutes*, and *Archaea-Chloroflexota*) and MeHg concentrations. Such correlative links between *hgcA* (gene or transcript) abundance and MeHg concentration and/or formation activity have been previously reported (19, 45, 46), but are not always observed, depending on the ecosystems (47, 48), as documented also for other metabolic processes (49).

A diverse community of *hgc*⁺ microorganisms is distributed along the redox gradient in the Black Sea

We demonstrate that not only the overall community but also the abundance and diversity of *hgc*⁺ microorganisms vary with the redox gradient in the water column of the Black Sea. The very low proportion of *hgc* genes detected in the oxic layer (and their taxonomic affiliation) is further discussed in Supplemental Information 3.1. Our findings showing a strong relation between oxygen depletion and *hgc*⁺ microorganism abundance are in line with previous studies in marine, brackish, and freshwater environments

(15, 17–19). We provide the first evidence for microbial potential to produce MeHg in the anoxic sulfidic waters of the Black Sea, as previously suggested by a modeling approach based on geochemical data (25). This disagrees with earlier studies where persistently high sulfide concentrations were believed to inhibit Hg methylation in the AOL of the Black Sea (24) and other systems (50, 51). Similar to our results, maximal methylation activity was also reported under sulfidic conditions in stratified brackish water (19) and a meromictic lake (52). The dual role of sulfide in Hg methylation is complex and still uncertain (51, 53).

Desulfobacterota members exhibit the highest diversity and abundances of *hgcA* genes in the Black Sea water column. The presence of *Desulfobacterota* in the anoxic water layer of the Black Sea can be explained by their metabolisms as sulfate reducers, iron reducers, and/or fermentative syntrophic in oxygen-deficient environments (54). Sulfate reduction has been previously reported in the Black Sea anoxic water (30, 55) and is also supported by our high HS⁻ concentrations in the AOL. For decades, *Desulfobacterota* members have been confirmed to be capable of Hg methylation and/or carrying *hgc* genes (3, 11). *Desulfobacterota* have also previously been identified as prevalent *hgc*⁺ microorganisms in many anoxic marine waters (17–19) and sediments (13, 56). In our work, certain *hgcA* genes belong to MAGs previously reconstructed from the Phoxy metagenomes (30). Among them, the *hgc*⁺ MAGs ^U*Desulfatibia profunda* NIOZ-UU30 and ^U*Desulfacyla* NIOZ-UU19, enriched in the anoxic waters, were described as probably having a strict sulfate-reducing lifestyle. By contrast, the *hgc*⁺ sulfate reducers ^U*Desulfacyla euxinica* NIOZ-UU27, ^U*Desulfatibia vada* NIOZ-UU17, and ^U*Desulfobacula maris* NIOZ-UU16, which were abundant in the suboxic waters and dominant at the top of the anoxic waters, feature a more flexible potential metabolism, with the ability to gain energy from the reduction of diverse electron acceptors (S⁰, thiosulfate, tetrathionate, nitrate, nitrite), possibly including oxygen respiration (30). The MAG of the SRB ^U*Desulfobiala pelagia* NIOZ-UU47, for which *hgcA* genes were found between 105 and 250 m, seems to have the ability to fix nitrogen. Altogether, these results show that *Desulfobacterota*-mediated MeHg formation in the Black Sea may be coupled to sulfate reduction but also to other metabolic pathways depending on the redox niche.

Certain *Anaerolineales* (*Chloroflexota*) are also part of the dominant *hgcA*-carriers in the suboxic and anoxic waters of the Black Sea including the MAGs NIOZ-UU11 and NIOZ-UU52. *Anaerolineales* are fermenters, in possible syntrophic association with methanogens (57). *Anaerolineales* MAGs were previously identified as highly abundant in the Black Sea, where some of them carried sulfate reduction genes (28). Although there is still limited genomic information about members of this group, a *hgc*⁺ MAG *Anaerolineales* representative (BSW_bin111) was detected in the anoxic brackish water of the Baltic Sea (19). In addition, *Phycisphaerae* (*Planctomycetota*), *Kiritimatiellales* (*Verrucomicrobiota*), and *Bacteroidales* (*Bacteroidota*) were identified as major potential Hg methylators in the oxygen-deficient waters of the Black Sea. Among these new, underappreciated, fermentative *hgcA* carriers, the *Bacteroidota* MAG NIOZ-UU65 was equipped with polysulfide reductase genes (30). *Phycisphaerales* have been identified in the euxinic waters of the Cariaco basin as attached to particles (58) and in the Black Sea (59) as potential degraders of newly formed OM not linked to the redox gradient (60), and some type strains seemed capable of nitrate reduction (61). *Phycisphaerales* have been reported as minor putative Hg methylator in marine sediments (13), salt marsh, and freshwater sediment (43). Culture and single-cell genomics of *Kiritimatiellales* representatives indicated a fermentative lifestyle, with the capacity for degradation of complex and recalcitrant polysaccharides and glycoproteins, as well as hydrolysis of sulfate esters, with wide oxygen and salinity tolerance, and a preference for biofilm habitats (62–65). *Kiritimatiellales* were previously identified by metagenomic approaches among the most prominent putative Hg methylators in sediment and anoxic water of eutrophic sulfate-rich freshwater lakes (14, 15) and in the anoxic brackish water of the Baltic Sea (19). Overall, fermenters from *Anaerolineales*, *Phycisphaerae*, *Kiritimatiellales*, and *Bacteroidales* have been rarely reported as putative Hg methylators, usually at low abundance in

ecosystems different from the present one. To our knowledge, this is the first report of their substantial joint contribution to Hg methylation, conforming a unique assemblage in a permanently stratified marine ecosystem. Among these diverse Hg methylators candidates found in the Black Sea suboxic/anoxic waters, some lineages (*Anaerolineales* and *Kiritimatiellales*) are common to other euxinic basins (17, 19), suggesting that they may be part of the important mediators of Hg methylation in permanently or not permanently anoxic water from marine and/or brackish environments with high sulfide concentrations. However, it is unclear if this diversity is a common trait of (not euxinic) OMZ, where Hg methylators have been rarely detected (10). Further studies should compare the *hgc*⁺ MAGs identified here and in similar oxygen-depleted marine systems, to explore the metabolic versatility of Hg-methylating microorganisms and their environmental drivers.

Finally, our results suggest that the qPCR estimates of *hgcA* genes identified by primers primarily designed to target *Archaea* are overestimated. This is supported by cloning-sequencing of PCR products obtained using *Archaea*-specific *hgcA* qPCR primers, showing that some amplicon sequences group with *Chloroflexota* rather than *Archaea* (Supplemental Information 1.4, Fig. S2). Additionally, our metagenome analyses consistently show that *hgc*⁺ *Chloroflexota* are major putative Hg methylation contributors, especially in the AOL, while *Archaea*-assigned *hgcA* are rare and not abundant (Data Sheet S1B and D). Recently, an analysis of publicly available MAGs revealed high similarities of *hgc* genes from *Euryarchaeota* and *Chloroflexota*, potentially due to horizontal gene transfers (9). Altogether, these results suggest that the *Archaea-hgcA* primers from Christensen et al. (37) are less specific than initially thought and likely include *hgcA* genes from other clades such as *Chloroflexota*.

Conclusion

Oxygen-limited and anoxic areas are spreading in the coastal and offshore ocean, implying modifications of biogeochemical cycles. The Black Sea offers a unique opportunity to study the effect of oxygen gradients on biogeochemical cycles such as Hg transformations. Our findings highlight that a unique combination of diverse dominant *hgc*⁺ microbes can coexist and jointly contribute to MeHg production in marine environments, with niche partitioning according to the redox gradient. We identified members of *Desulfobacterota*, *Chloroflexota*, *Verrucomicrobiota*, *Planctomycetota*, and *Bacteroidota* as the main actors of Hg methylation in the Black Sea water column. The microbial communities, including putative Hg methylators, were horizontally homogeneous across the Black Sea, but vertically stratified. The abundance of *hgcA* genes increased with depth, being positively correlated with MeHg concentration and negatively with oxygen concentration. Our DNA-based results support that Hg methylation potentially occurs predominantly in the anoxic waters of the Black Sea, which should be further confirmed by measuring gene expression and/or methylation rates. Microorganisms harboring *hgc*⁺ were dominated by *Desulfobacterota*, followed by a high diversity of previously less recognized Hg methylators belonging to *Phycisphaerae*, *Kiritimatiellales*, and *Anaerolineales*. The strong environmental gradients across the Black Sea water column affect the microbial community composition, resulting in a partitioning of Hg-methylating microorganisms, and their associated metabolic pathways, differing across redox niches. Our results, robustly validated by two different methodological approaches (qPCR and metagenomics), were consistent with measured environmental parameters, including MeHg concentration. By identifying marine anoxic niches as a primary MeHg source, this study is of major relevance in the context of global warming and anthropogenic activity which currently result in enhanced seawater deoxygenation and global expansion of anoxic zones.

ACKNOWLEDGMENTS

This study was financially supported by the French National Research Institute for Sustainable Development (IRD) through the M.I.O. internal grant "ACTION SUD-Commet"

(L. Cabrol), the Severo Ochoa Excellence Program postdoctoral fellowship awarded in 2021 to Eric Capo (CEX2019-000928-S), and the Ramón y Cajal program (RYC2019-028400-I, AEI Spain) awarded to Andrea G. Bravo. We acknowledge the Dutch funding agency (project number: 822.01.015) of the national science foundation NWO for funding this work as part of GEOTRACES. L.-E.H.-B.'s work was supported by research grant ERC-2010-StG_20091028 from the European Research Council.

We thank the chief scientists of the MEDBlack cruise, M. J. A. Rijkenberg, L. J. A. Gerringa, and the shipboard party for their support. A special thanks goes to Matthew Patey for handling the *in situ* pumps. We thank Sophie Guasco at the M.I.O. for technical support with cloning sequencing of *hgcA* genes. The computations were performed on resources provided by the Swedish Research Council (grants to S.B.) and SNIC through Uppsala Multidisciplinary Center for Advanced Computational Science (UPPMAX) using the compute project SNIC 2021/5-53.

The authors have no competing interests to declare.

AUTHOR AFFILIATIONS

¹Aix Marseille University, Univ. Toulon, CNRS, IRD, Mediterranean Institute of Oceanography (MIO) UM 110, Marseille, France

²Institute of Ecology and Biodiversity (IEB), University of Chile, Santiago, Chile

³Department of Marine Biology and Oceanography, Institute of Marine Sciences, CSIC, Barcelona, Spain

⁴Department of Aquatic Sciences and Assessment, Swedish University of Agricultural Sciences, Uppsala, Sweden

⁵Department of Ecology and Environmental Science, Umeå University, Umeå, Sweden

⁶Laboratory of Microbiology, Wageningen University and Research, Wageningen, the Netherlands

⁷Wageningen Food and Biobased Research, Wageningen, the Netherlands

⁸Department of Marine Microbiology and Biogeochemistry, NIOZ Royal Netherlands Institute for Sea Research, Texel, the Netherlands

⁹Faculty of Geosciences, Department of Earth Sciences, Utrecht University, Utrecht, the Netherlands

¹⁰Department of Chemistry, Umeå University, Umeå, Sweden

AUTHOR ORCIDs

Léa Cabrol  <http://orcid.org/0000-0003-0417-2021>

Eric Capo  <http://orcid.org/0000-0001-9143-7061>

F. A. Bastiaan von Meijenfildt  <http://orcid.org/0000-0002-0037-0007>

Stefan Bertilsson  <https://orcid.org/0000-0002-4265-1835>

Laura Villanueva  <http://orcid.org/0000-0001-5659-8599>

Irene Sánchez-Andrea  <http://orcid.org/0000-0001-6977-3026>

FUNDING

| Funder | Grant(s) | Author(s) |
|--|---|------------------|
| Institut de Recherche pour le Développement (IRD) | M.I.O internal grant "ACTION SUD-Commet" | Léa Cabrol |
| Fundación Carmen y Severo Ochoa (Carmen and Severo Ochoa Foundation) | Excellence Program postdoctoral fellowship CEX2019-000928-S | Eric Capo |
| MEC Agencia Estatal de Investigación (AEI) | Ramón y Cajal program (RYC2019-028400-I) | Andrea G. Bravo |
| Nederlandse Organisatie voor Wetenschappelijk Onderzoek (NWO) | GEOTRACES project number: 822.01.015 | Laura Villanueva |

| Funder | Grant(s) | Author(s) |
|--------------------------------------|-----------------------|------------------------------|
| EC European Research Council (ERC) | ERC-2010-StG_20091028 | Lars-Eric Heimbürger Boavida |

AUTHOR CONTRIBUTIONS

Léa Cabrol, Conceptualization, Data curation, Formal analysis, Investigation, Methodology, Visualization, Writing – original draft, Writing – review and editing | Eric Capo, Data curation, Formal analysis, Investigation, Methodology, Visualization, Writing – original draft, Writing – review and editing | Daan M. van Vliet, Data curation, Formal analysis, Investigation, Validation, Writing – review and editing | F. A. Bastiaan von Meijenfheldt, Data curation, Investigation, Validation, Writing – review and editing | Stefan Bertilsson, Data curation, Investigation, Writing – review and editing, Validation | Laura Villanueva, Conceptualization, Writing – review and editing, Validation, Funding acquisition, Project administration, Resources | Irene Sánchez-Andrea, Data curation, Investigation, Writing – review and editing | Erik Björn, Data curation, Investigation, Writing – review and editing, Validation, Resources | Andrea G. Bravo, Investigation, Methodology, Writing – review and editing, Validation, Supervision | Lars-Eric Heimbürger Boavida, Conceptualization, Formal analysis, Investigation, Methodology, Writing – review and editing, Validation, Funding acquisition, Resources, Supervision

DATA AVAILABILITY

Raw sequences have been deposited at NCBI GenBank, SRA database, under the BioProject accession number [PRJNA895066](https://www.ncbi.nlm.nih.gov/bioproject/PRJNA895066).

ADDITIONAL FILES

The following material is available [online](#).

Supplemental Material

Supplemental Information (mSystems.00537-23-s0001.docx). Table S1, supplemental text, and Figure S1 to S4.

Data Sheet (mSystems.00537-23-s0002.xlsx). Environmental and molecular data from both cruises, OTU abundance table and taxonomy, *hgcA* and *hgcB* genes found in Phoxy cruise metagenomes, and community composition.

REFERENCES

1. Outridge PM, Mason RP, Wang F, Guerrero S, Heimbürger-Boavida LE. 2018. Updated global and oceanic mercury budgets for the United Nations global mercury assessment 2018. *Environ Sci Technol* 52:11466–11477. <https://doi.org/10.1021/acs.est.8b01246>
2. Zhang Y, Song Z, Huang S, Zhang P, Peng Y, Wu P, Gu J, Dutkiewicz S, Zhang H, Wu S, Wang F, Chen L, Wang S, Li P. 2021. Global health effects of future atmospheric mercury emissions. *Nat Commun* 12:3035. <https://doi.org/10.1038/s41467-021-23391-7>
3. Bravo AG, Cosío C. 2020. Biotic formation of methylmercury: a biophysico-chemical conundrum. *Limnol Oceanogr* 65:1010–1027. <https://doi.org/10.1002/lno.11366>
4. Heimbürger L-E, Cossa D, Marty J-C, Migon C, Averty B, Dufour A, Ras J. 2010. Methyl mercury distributions in relation to the presence of nano- and picophytoplankton in an oceanic water column (Ligurian Sea, North-Western Mediterranean). *Geochim Cosmochim Acta* 74:5549–5559. <https://doi.org/10.1016/j.gca.2010.06.036>
5. Soerensen AL, Schartup AT, Skrobonja A, Bouchet S, Amouroux D, Liem-Nguyen V, Björn E. 2018. Deciphering the role of water column redoxclines on methylmercury cycling using speciation modeling and observations from the Baltic Sea. *Global Biogeochem Cycles* 32:1498–1513. <https://doi.org/10.1029/2018GB005942>
6. Yu R-Q, Barkay T. 2022. Microbial mercury transformations: molecules, functions and organisms. *Adv Appl Microbiol* 118:31–90. <https://doi.org/10.1016/bs.aambs.2022.03.001>
7. Parks JM, Johs A, Podar M, Bridou R, Hurt RA, Smith SD, Tomanicek SJ, Qian Y, Brown SD, Brandt CC, Palumbo AV, Smith JC, Wall JD, Elias DA, Liang L. 2013. The genetic basis for bacterial mercury methylation. *Science* 339:1332–1335. <https://doi.org/10.1126/science.1230667>
8. Capo E, Peterson BD, Kim M, Jones DS, Acinas SG, Amyot M, Bertilsson S, Björn E, Buck M, Cosío C, Elias DA, Gilmour C, Goñi-Urriza M, Gu B, Lin H, Liu Y-R, McMahon K, Moreau JW, Pinhassi J, Podar M, Puente-Sánchez F, Sánchez P, Storck V, Tada Y, Vigneron A, Walsh DA, Vandewalle-Capo M, Bravo AG, Gionfriddo CM. 2023. A consensus protocol for the recovery of mercury methylation genes from metagenomes. *Mol Ecol Resour* 23:190–204. <https://doi.org/10.1111/1755-0998.13687>
9. McDaniel EA, Peterson BD, Stevens SLR, Tran PQ, Anantharaman K, McMahon KD. 2020. Expanded phylogenetic diversity and metabolic flexibility of mercury-methylating microorganisms. *mSystems* 5:e00299-20. <https://doi.org/10.1128/mSystems.00299-20>
10. Podar M, Gilmour CC, Brandt CC, Soren A, Brown SD, Crable BR, Palumbo AV, Somenahally AC, Elias DA. 2015. Global prevalence and distribution of genes and microorganisms involved in mercury methylation. *Sci Adv* 1:e1500675. <https://doi.org/10.1126/sciadv.1500675>

11. Gilmour CC, Podar M, Bullock AL, Graham AM, Brown SD, Somenahally AC, Johs A, Hurt RA, Bailey KL, Elias DA. 2013. Mercury methylation by novel microorganisms from new environments. *Environ Sci Technol* 47:11810–11820. <https://doi.org/10.1021/es403075t>
12. Gilmour CC, Bullock AL, McBurney A, Podar M, Elias DA. 2018. Robust mercury methylation across diverse methanogenic *Archaea*. *mBio* 9:e02403-17. <https://doi.org/10.1128/mBio.02403-17>
13. Capo E, Broman E, Bonaglia S, Bravo AG, Bertilsson S, Soerensen AL, Pinhassi J, Lundin D, Buck M, Hall POJ, Nascimento FJA, Björn E. 2022. Oxygen-deficient water zones in the Baltic Sea promote uncharacterized Hg methylating microorganisms in underlying sediments. *Limnology & Oceanography* 67:135–146. <https://doi.org/10.1002/lno.11981>
14. Jones DS, Walker GM, Johnson NW, Mitchell CPJ, Coleman Wasik JK, Bailey JV. 2019. Molecular evidence for novel mercury methylating microorganisms in sulfate-impacted lakes. *ISME J* 13:1659–1675. <https://doi.org/10.1038/s41396-019-0376-1>
15. Peterson BD, McDaniel EA, Schmidt AG, Lepak RF, Janssen SE, Tran PQ, Marick RA, Ogorek JM, DeWild JF, Krabbenhoft DP, McMahon KD. 2020. Mercury methylation genes identified across diverse anaerobic microbial guilds in a eutrophic sulfate-enriched lake. *Environ Sci Technol* 54:15840–15851. <https://doi.org/10.1021/acs.est.0c05435>
16. Vigneron A, Cruaud P, Aubé J, Guyoneaud R, Goñi-Urriza M. 2021. Transcriptomic evidence for versatile metabolic activities of mercury cycling microorganisms in brackish microbial mats. *NPJ Biofilms Microbiomes* 7:83. <https://doi.org/10.1038/s41522-021-00255-y>
17. Lin H, Ascher DB, Myung Y, Lamborg CH, Hallam SJ, Gionfriddo CM, Holt KE, Moreau JW. 2021. Mercury methylation by metabolically versatile and cosmopolitan marine bacteria. *ISME J* 15:1810–1825. <https://doi.org/10.1038/s41396-020-00889-4>
18. Capo E, Bravo AG, Soerensen AL, Bertilsson S, Pinhassi J, Feng C, Andersson AF, Buck M, Björn E. 2020. Deltaproteobacteria and spirochaetes-like bacteria are abundant putative mercury methylators in oxygen-deficient water and marine particles in the Baltic sea. *Front Microbiol* 11:574080. <https://doi.org/10.3389/fmicb.2020.574080>
19. Capo E, Feng C, Bravo AG, Bertilsson S, Soerensen AL, Pinhassi J, Buck M, Karlsson C, Hawkes J, Björn E. 2022. Expression levels of *hgcAB* genes and mercury availability jointly explain methylmercury formation in stratified brackish waters. *Environ Sci Technol* 56:13119–13130. <https://doi.org/10.1021/acs.est.2c03784>
20. Breitung D, Levin LA, Oschlies A, Grégoire M, Chavez FP, Conley DJ, Garçon V, Gilbert D, Gutiérrez D, Isensee K, Jacinto GS, Limburg KE, Montes I, Naqvi SWA, Pitcher GC, Rabalais NN, Roman MR, Rose KA, Seibel BA, Telszewski M, Yasuhara M, Zhang J. 2018. Declining oxygen in the global ocean and coastal waters. *Science* 359:1–11. <https://doi.org/10.1126/science.aam7240>
21. Wakeham SG. 2020. Organic biogeochemistry in the oxygen-deficient ocean: a review. *Organic Geochemistry* 149:104096. <https://doi.org/10.1016/j.orggeochem.2020.104096>
22. Jürgens K, Taylor GT. 2018. Microbial ecology and biogeochemistry of oxygen-deficient water columns, p 231–288. In Gasol J, D Kirchman (ed), *Microbial ecology of the oceans*. John Wiley & Sons, Inc.
23. Glazer BT, Luther GW, Konovalov SK, Friederich GE, Trouwborst RE, Romanov AS. 2006. Spatial and temporal variability of the Black Sea suboxic zone. *Deep-Sea Res II: Top Stud Oceanogr* 53:1756–1768. <https://doi.org/10.1016/j.dsr2.2006.03.022>
24. Lamborg CH, Yiğiterhan O, Fitzgerald WF, Balcom PH, Hammerschmidt CR, Murray J. 2008. Vertical distribution of mercury species at two sites in the Western Black Sea. *Marine Chemistry* 111:77–89. <https://doi.org/10.1016/j.marchem.2007.01.011>
25. Rosati G, Heimbürger LE, Melaku Canu D, Lagane C, Laffont L, Rijkenberg MJA, Gerringa LJA, Solidoro C, Gencarelli CN, Hedgecock IM, De Baar HJW, Sonke JE. 2018. Mercury in the Black Sea: new insights from measurements and numerical modeling. *Global Biogeochem Cycles* 32:529–550. <https://doi.org/10.1002/2017GB005700>
26. Zhang Y, Pavlovska M, Stoica E, Prekrasna I, Yang J, Slobodnik J, Zhang X, Dykji E. 2020. Holistic pelagic biodiversity monitoring of the Black Sea via eDNA metabarcoding approach: from bacteria to marine mammals. *Environ Int* 135:105307. <https://doi.org/10.1016/j.envint.2019.105307>
27. Zatsepin AG. 2003. Observations of Black Sea mesoscale eddies and associated horizontal mixing. *J Geophys Res* 108:1–27. <https://doi.org/10.1029/2002JC001390>
28. Cabello-Yeves PJ, Callieri C, Picazo A, Mehrshad M, Haro-Moreno JM, Roda-García JJ, Dzhenbekova N, Slabakova V, Slabakova N, Moncheva S, Rodríguez-Valera F. 2021. The microbiome of the Black Sea water column analyzed by shotgun and genome centric metagenomics. *Environ Microbiome* 16:5. <https://doi.org/10.1186/s40793-021-00374-1>
29. Suominen S, Dombrowski N, Sinninghe Damsté JS, Villanueva L. 2021. A diverse uncultivated microbial community is responsible for organic matter degradation in the Black Sea sulphidic zone. *Environ Microbiol* 23:2709–2728. <https://doi.org/10.1111/1462-2920.14902>
30. van Vliet DM, von Meijenfheldt FAB, Dutilh BE, Villanueva L, Sinninghe Damsté JS, Stams AJM, Sánchez-Andrea I. 2021. The bacterial sulfur cycle in expanding dysoxic and euxinic marine waters. *Environ Microbiol* 23:2834–2857. <https://doi.org/10.1111/1462-2920.15265>
31. Villanueva L, von Meijenfheldt FAB, Westbye AB, Yadav S, Hopmans EC, Dutilh BE, Damsté JSS. 2021. Bridging the membrane lipid divide: bacteria of the FCB group superphylum have the potential to synthesize archaeal ether lipids. *ISME J* 15:168–182. <https://doi.org/10.1038/s41396-020-00772-2>
32. Stewart K, Kassakian S, Krynytzky M, DiJulio D, Murray JW. 2007. Oxidic, Suboxic, and Anoxic conditions in the black sea, p 1–22. In Yankov-Hombach V, AS Gilbert, N Panin, P Dolukhanov (ed), *The Black Sea flood question: changes in coastline, climate, and settlement human*. Springer. <https://doi.org/10.1007/978-1-4020-5302-3>
33. Sollai M, Villanueva L, Hopmans EC, Reichart G-J, Sinninghe Damsté JS. 2019. A combined lipidomic and 16S rRNA gene amplicon sequencing approach reveals archaeal sources of intact polar lipids in the stratified Black Sea water column. *Geobiology* 17:91–109. <https://doi.org/10.1111/gbi.12316>
34. Wang Y, Qian P-Y, Field D. 2009. Conservative fragments in bacterial 16S rRNA genes and primer design for 16S ribosomal DNA amplicons in metagenomic studies. *PLoS ONE* 4:e7401. <https://doi.org/10.1371/journal.pone.0007401>
35. Schwob G, Cabrol L, Poulin E, Orlando J. 2020. Characterization of the gut microbiota of the antarctic heart urchin (spatangoida) *Abatus agassizii*. *Front Microbiol* 11:308. <https://doi.org/10.3389/fmicb.2020.00308>
36. Mahé F, Czeck L, Stamatakis A, Quince C, de Vargas C, Dunthorn M, Rognes T. 2021. Swarm v3: towards tera-scale amplicon clustering. *Bioinformatics* 38:267–269. <https://doi.org/10.1093/bioinformatics/btab493>
37. Christensen GA, Wymore AM, King AJ, Podar M, Hurt RA, Santillan EU, Soren A, Brandt CC, Brown SD, Palumbo AV, Wall JD, Gilmour CC, Elias DA. 2016. Development and validation of broad-range qualitative and clade-specific quantitative molecular probes for assessing mercury methylation in the environment. *Appl Environ Microbiol* 82:6068–6078. <https://doi.org/10.1128/AEM.01271-16>
38. Gionfriddo CM, Capo E, Peterson B, Lin H, Jones D, Bravo AG, Bertilsson S, Moreau J, McMahon K, Elias D, Gilmour C. 2021. Hg-MATE-dB.V1.01142021. Hg-Cycling Microorg. Aquat Terr Ecosyst database.
39. Finn RD, Clements J, Eddy SR. 2011. HMMER web server: interactive sequence similarity searching. *Nucleic Acids Res* 39:W29–W37. <https://doi.org/10.1093/nar/gkr367>
40. Matsen FA, Kodner RB, Armbrust EV. 2010. Pplacer: linear time maximum-likelihood and Bayesian phylogenetic placement of sequences onto a fixed reference tree. *BMC Bioinformatics* 11:538. <https://doi.org/10.1186/1471-2105-11-538>
41. Ozturk RC, Altinok I, Feyzioglu AM, Capkin E, Yildiz I. 2021. Influence of the depth and season on microbial community dynamics of the black sea. *Res sq*. <https://doi.org/10.21203/rs.3.rs-693853/v1>
42. Christensen GA, Gionfriddo CM, King AJ, Moberly JG, Miller CL, Somenahally AC, Callister SJ, Brewer H, Podar M, Brown SD, Palumbo AV, Brandt CC, Wymore AM, Brooks SC, Hwang C, Fields MW, Wall JD, Gilmour CC, Elias DA. 2019. Determining the reliability of measuring mercury cycling gene abundance with correlations with mercury and methylmercury concentrations. *Environ Sci Technol* 53:8649–8663. <https://doi.org/10.1021/acs.est.8b06389>
43. Gionfriddo CM, Wymore AM, Jones DS, Wilpieszski RL, Lynes MM, Christensen GA, Soren A, Gilmour CC, Podar M, Elias DA. 2020. An improved *hgcAB* primer set and direct high-throughput sequencing expand Hg-methylator diversity in nature. *Front Microbiol* 11:541554. <https://doi.org/10.3389/fmicb.2020.541554>

44. Roth S, Poulin BA, Baumann Z, Liu X, Zhang L, Krabbenhoft DP, Hines ME, Schaefer JK, Barkay T. 2021. Nutrient inputs stimulate mercury methylation by syntrophs in a subarctic peatland. *Front Microbiol* 12:741523. <https://doi.org/10.3389/fmicb.2021.741523>
45. Vishnivetskaya TA, Hu H, Van Nostrand JD, Wymore AM, Xu X, Qiu G, Feng X, Zhou J, Brown SD, Brandt CC, Podar M, Gu B, Elias DA. 2018. Microbial community structure with trends in methylation gene diversity and abundance in mercury-contaminated rice paddy soils in Guizhou, China. *Environ Sci Process Impacts* 20:673–685. <https://doi.org/10.1039/c7em00558j>
46. Peterson BD, Krabbenhoft DP, McMahon KD, Ogorek JM, Tate MT, Orem WH, Poulin BA. 2023. Environmental formation of methylmercury is controlled by synergy of inorganic mercury bioavailability and microbial mercury-methylation capacity. *Environ Microbiol*:1–15. <https://doi.org/10.1111/1462-2920.16364>
47. Bravo AG, Loizeau J-L, Dranguet P, Makri S, Björn E, Ungureanu VG, Slaveykova VI, Cosio C. 2016. Persistent Hg contamination and occurrence of Hg-methylating transcript (hgcA) downstream of a chlor-alkali plant in the Olt River (Romania). *Environ Sci Pollut Res Int* 23:10529–10541. <https://doi.org/10.1007/s11356-015-5906-4>
48. Christensen GA, Somenahally AC, Moberly JG, Miller CM, King AJ, Gilmour CC, Brown SD, Podar M, Brandt CC, Brooks SC, Palumbo AV, Wall JD, Elias DA. 2018. Carbon amendments alter microbial community structure and net mercury methylation potential in sediments. *Appl Environ Microbiol* 84:e01049-17. <https://doi.org/10.1128/AEM.01049-17>
49. Rocca JD, Hall EK, Lennon JT, Evans SE, Waldrop MP, Cotner JB, Nemergut DR, Graham EB, Wallenstein MD. 2015. Relationships between protein-encoding gene abundance and corresponding process are commonly assumed yet rarely observed. *ISME J* 9:1693–1699. <https://doi.org/10.1038/ismej.2014.252>
50. Benoit JM, Gilmour CC, Mason RP, Heyes A. 1999. Sulfide controls on mercury speciation and bioavailability to methylating bacteria in sediment pore waters. *Environ Sci Technol* 33:951–957. <https://doi.org/10.1021/es9808200>
51. Hsu-Kim H, Kucharzyk KH, Zhang T, Deshusses MA. 2013. Mechanisms regulating mercury bioavailability for methylating microorganisms in the aquatic environment: a critical review. *Environ Sci Technol* 47:2441–2456. <https://doi.org/10.1021/es304370g>
52. Tisserand D, Guédron S, Viollier E, Jézéquel D, Rigaud S, Campillo S, Sarret G, Charlet L, Cossa D. 2022. Mercury, organic matter, iron, and sulfur co-cycling in a ferruginous meromictic lake. *Appl Geochem* 146:105463. <https://doi.org/10.1016/j.apgeochem.2022.105463>
53. Regnell O, Watras CJ. 2019. Microbial mercury methylation in aquatic environments: a critical review of published field and laboratory studies. *Environ Sci Technol* 53:4–19. <https://doi.org/10.1021/acs.est.8b02709>
54. Waite DW, Chuvochina M, Pelikan C, Parks DH, Yilmaz P, Wagner M, Loy A, Naganuma T, Nakai R, Whitman WB, Hahn MW, Kuever J, Hugenholtz P. 2020. Proposal to reclassify the proteobacterial classes *Deltaproteobacteria* and *Oligoflexia*, and the phylum *Thermodesulfobacteria* into four phyla reflecting major functional capabilities. *Int J Syst Evol Microbiol* 70:5972–6016. <https://doi.org/10.1099/ijsem.0.004213>
55. Neretin LN, Volkov II, Böttcher ME, Grinenko VA. 2001. A sulfur budget for the black sea anoxic zone. *Deep-Sea Res I: Oceanogr Res Pap* 48:2569–2593. [https://doi.org/10.1016/S0967-0637\(01\)00030-9](https://doi.org/10.1016/S0967-0637(01)00030-9)
56. Azaroff A, Goñi Urriza M, Gassie C, Monperrus M, Guyoneaud R. 2020. Marine mercury-methylating microbial communities from coastal to Capbreton Canyon sediments (North Atlantic ocean). *Environ Pollut* 262:114333. <https://doi.org/10.1016/j.envpol.2020.114333>
57. Sekiguchi Y, Yamada T, Hanada S, Ohashi A, Harada H, Kamagata Y. 2003. *Anaerolinea thermophila* gen. nov., sp. nov. and *Caldilinea aerophila* gen. nov., sp. nov., novel filamentous thermophiles that represent a previously uncultured lineage of the domain *Bacteria* at the subphylum level. *Int J Syst Evol Microbiol* 53:1843–1851. <https://doi.org/10.1099/ijms.0.02699-0>
58. Suter EA, Pachiadaki M, Taylor GT, Astor Y, Edgcomb VP. 2018. Free-living chemoautotrophic and particle-attached heterotrophic prokaryotes dominate microbial assemblages along a pelagic redox gradient. *Environ Microbiol* 20:693–712. <https://doi.org/10.1111/1462-2920.13997>
59. Fuchsman CA, Staley JT, Oakley BB, Kirkpatrick JB, Murray JW. 2012. Free-living and aggregate-associated planctomycetes in the black sea. *FEMS Microbiol Ecol* 80:402–416. <https://doi.org/10.1111/j.1574-6941.2012.01306.x>
60. Suominen S, Gomez - Saez GV, Dittmar T, Sinninghe Damsté JS, Villanueva L. 2022. Interplay between microbial community composition and chemodiversity of dissolved organic matter throughout the black sea water column redox gradient. *Limnology & Oceanography* 67:329–347. <https://doi.org/10.1002/lno.11995>
61. Fukunaga Y, Kurahashi M, Sakiyama Y, Ohuchi M, Yokota A, Harayama S. 2009. *Phycisphaera mikurensis* gen. nov., sp. nov., isolated from a marine alga, and proposal of *Phycisphaeraeaceae* fam. nov., *Phycisphaerales* ord. nov. and *Phycisphaerae* classis nov. in the phylum *Planctomycetes*. *J Gen Appl Microbiol* 55:267–275. <https://doi.org/10.2323/jgam.55.267>
62. Sackett JD, Kruger BR, Becraft ED, Jarett JK, Stepanauskas R, Woyke T, Moser DP. 2019. Four draft single-cell genome sequences of novel, nearly identical *Kiritimatiella* strains isolated from the continental deep subsurface. *Microbiol Resour Announc* 8:e01249-18. <https://doi.org/10.1128/MRA.01249-18>
63. Spring S, Bunk B, Spröer C, Schumann P, Rohde M, Tindall BJ, Klenk H-P. 2016. Characterization of the first cultured representative of *Verrucomicrobia* subdivision 5 indicates the proposal of a novel phylum. *ISME J* 10:2801–2816. <https://doi.org/10.1038/ismej.2016.84>
64. van Vliet DM, Lin Y, Bale NJ, Koenen M, Villanueva L, Stams AJM, Sánchez-Andrea I. 2020. *Pontiella desulfatans* gen. nov., sp. nov., and *pontiella sulfatireligans* sp. nov., two marine anaerobes of the pontiellaceae fam. nov. producing sulfated glycosaminoglycan-like exopolymers. *Microorganisms* 8:1–22. <https://doi.org/10.3390/microorganisms8060920>
65. van Vliet DM, Palakawong Na Ayudthaya S, Diop S, Villanueva L, Stams AJM, Sánchez-Andrea I. 2019. Anaerobic degradation of sulfated polysaccharides by two novel *Kiritimatiellales* strains isolated from black sea sediment. *Front Microbiol* 10:253. <https://doi.org/10.3389/fmicb.2019.00253>